# Articles

## Chemistry of Azoimidazoles: Synthesis, Spectral Characterization, Electrochemical Studies, and X-ray Crystal Structures of Isomeric Dichloro Bis[1-alkyl-2-(arylazo)imidazole] Complexes of Ruthenium(II)

**Tarun Kumar Misra,[†] Debasis Das,[†] Chittaranjan Sinha,*[,†] Prasanta Ghosh,[‡] and Chandan Kumar Pal[‡]**

Department of Chemistry, The University of Burdwan, Burdwan 713 104, India, and Department of Inorganic Chemistry, Indian Association for the Cultivation of Science, Calcutta 700 032, India

*Received April 16, 1997*

Several new ligands, azoimidazoles belonging to the class 1-methyl-2-(arylazo)imidazoles ($L_1$ (**3**)) and 1-benzyl-2-(arylazo)imidazoles ($L_2$ (**4**)) (R = H (**a**), Me (**b**), OMe (**c**), Cl (**d**), $NO_2$ (**e**)) have been synthesized and reacted with $RuCl_3$ in ethanol under refluxing conditions. Two isomers of the composition $RuL_2Cl_2$, green (i) and blue (iii), are chromatographically separated. The green isomer is quantitatively transformed to the blue isomer on refluxing in a high boiling solvent. The isomeric structures have been confirmed by X-ray crystallography. Crystal data are as follows. Green complex $C_{38}H_{34}Cl_2N_8Ru$ (**6a**): crystal system monoclinic; space group $C2/c$; $a$ = 15.680(8) Å; $b$ = 22.766(14) Å; $c$ = 11.473(5) Å; $\beta$ = 119.27(4)°; $V$ = 3573(3) Å$^3$ $Z$ = 4; $R$ = 3.59%; $R_w$ = 4.38%. Blue complex $C_{22}H_{24}Cl_2N_8Ru$ (**7b**): crystal system monoclinic; space group $P2_1/n$, $a$ = 9.547(6) Å; $b$ = 22.554(14) Å; $c$ = 11.748(8) Å; $\beta$ = 99.07(5)°; $V$ = 2498(3) Å$^3$; $Z$ = 4; $R$ = 3.15%; $R_w$ = 4.51%. With reference to the pairs of Cl, N(imidazole), and N(azo) bound to Ru, the green isomer (**6a**) has a *trans*−cis−*cis* configuration and the blue isomer (**7b**) is *cis*−*trans*−*cis*. In both structures the Ru−N(azo) distances are relatively shorter than Ru−N(imidazole), indicating stronger bonding in the former and the presence of a Ru−L $\pi$-interaction that is localized in the Ru−azo fragment. The isomer configuration is supported by IR and $^1$H NMR data. The compounds exhibit $t_2$(Ru) → $\pi^*$(L) MLCT transitions in the visible region. Redox studies show the Ru(III)/Ru(II) couple in the green complexes (**5**, **6**) at 0.6−0.7 V and in the blue complexes at 0.7−0.8 V *versus* SCE and two successive azo reductions. The difference in the first metal and ligand redox potentials is linearly correlated with $\nu_{CT}$ ($t_2$(Ru) → $\pi^*$(L).

### Introduction

The ruthenium chemistry of unsaturated nitrogenous ligands has developed[1−10] in recent times, primarily due to the wide range of oxidation states, varieties of reactivities of the complexes, directional electron and energy transfer, light-to-electrical energy conversion, photophysical and photochemical

[†] The University of Burdwan.
[‡] Indian Association for the Cultivation of Science.

(1) (a) Reedijk, J. In *Comprehensive Coordination Chemistry*; Wilkinson, G., McCleverty, J. A., Eds.; Pergamon: Oxford, U.K., 1987; Vol. 2, p 43. (b) Wong, W. T. *Coord. Chem. Rev.* **1994**, *131*, 45. (c) Seddon, E. A.; Seddon, K. R. *The Chemistry of Ruthenium*; Elsevier: Amsterdam, 1984.
(2) (a) Eggleston, D. S.; Goldsby, K. A.; Hodgson, D. J.; Meyer, T. J. *Inorg. Chem.* **1985**, *24*, 4573. (b) de Klerk-Engles, B.; Frawhauf, H. W.; Vrieze, K.; Koojiman, H.; Spek, A. L. *Inorg. Chem.* **1993**, *32*, 5528. (c) Bassel, C. A.; Margarucci, J. A.; Acquaye, J. H.; Rubino, R. S.; Crandall, J.; Jrircitano, A. J.; Takuchi, K. J. *Inorg. Chem.* **1993**, *32*, 5779. (d) Rudi, A.; Kashman, Y.; Gut, D.; Lellouche, F.; Kol, M. *J. Chem. Soc., Chem. Commun.* **1997**, 17. (e) Beer, P. D.; Dent, S. W.; Hobbs, G. S.; Wear, J. J. *J. Chem. Soc., Chem. Commun.* **1997**, 99.
(3) Kalyansundaram, K.; Lakeeruddin, M. S.; Nazeeruddin, M. K. *Coord. Chem. Rev.* **1994**, *132*, 259. Kalyansundaram, K. *Coord. Chem. Rev.* **1982**, *46*, 159.
(4) Ghosh, B. K.; Chakravorty, A. *Coord. Chem. Rev.* **1989**, *95*, 239.
(5) Santra, B. K.; Thakur, G. A.; Ghosh, P.; Pramanik, K. A.; Lahiri, G. K. *Inorg. Chem.* **1996**, *35*, 3050. Chakravorty, J.; Bhattacharya, S., *Transition Met. Chem.* **1995**, *20*, 138. Mallik, T. K.; Das, P. K.; Roy, B. K.; Ghosh, B. K. *J. Chem. Res. (S)* **1993**, 374. Kakoti, M.; Chaudhury, S.; Deb, A. K.; Goswami, S. *Polyhedron* **1993**, *12*, 783.
(6) Krause, R. A.; Krause, K. *Inorg. Chem.* **1984**, *23*, 2195; **1982**, *21*, 1714; **1980**, *19*, 2600.
(7) (a) Bag, N.; Lahiri, G. K.; Chakravorty, A. *Inorg. Chem.* **1992**, *31*, 40. (b) Lahiri, G. K.; Bhattacharya, S.; Goswami, S.; Chakravorty, A. *J. Chem. Soc., Dalton Trans.* **1990**, 561. (c) Lahiri, G. K.; Goswami, S.; Falvello, L. R.; Chakravorty, A. *Inorg. Chem.* **1987**, *26*, 3365. (d) Mahapatra, A. K.; Ghosh, B. K.; Goswami, S.; Chakravorty, A. *J. Indian Chem. Soc.* **1986**, *63*, 101. (e) Ghosh, P.; Chakravorty, A. *J. Chem. Soc., Dalton Trans.* **1985**, 361. (f) Seal, A.; Ray, S. *Acta Crystallogr., Sect. C: Struct. Commun.* **1984**, *C40*, 929. (g) Goswami, S.; Mukherjee, R. N.; Chakravorty, A. *Inorg. Chem.* **1983**, *22*, 2825. (h) Goswami, S.; Chakravorty, A. R.; Chakravorty, A. *Inorg. Chem.* **1983**, *22*, 602. (i) Goswami, S.; Chakravorty, A.; Chakravorty, A. *J. Chem. Soc., Chem. Commun.* **1982**, 1288. (j) Goswami, S.; Chakravorty, A.; Chakravorty, A. *Inorg. Chem.* **1981**, *20*, 2246.
(8) (a) Ghosh, B. K.; Goswami, S.; Chakravorty, A. *Inorg. Chem.* **1983**, *22*, 3358. (b) Ghosh, B. K.; Mukhopadhyay, A.; Goswami, S.; Ray, S.; Chakravorty, A. *Inorg. Chem.* **1984**, *23*, 4633.
(9) Argazzi, R.; Bignozzi, C. A.; Heimer, T. A.; Meyer, G. J. *Inorg. Chem.* **1997**, *36*, 2. Hung, C. Y.; Wang, T. L.; Jang, Y.; Kim, W. Y.; Schmekl, K. L.; Thumel, R. P. *Inorg. Chem.* **1996**, *35*, 5953. Chen, X. M.; Zang, W. H.; Chen, J.; Yang, Y. S.; Gang, M. L. *J. Chem. Soc., Dalton Trans.* **1996**, 1767. Real, A.; Munoz, M. C.; Andress, F.; Granier, T.; Gallos, B. *Inorg. Chem.* **1994**, *33*, 3587.

S0020-1669(97)00446-1 CCC: $15.00 
Published on Web 03/31/1998

properties, DNA intercalation, and ability to serve as building blocks in supramolecular arrays. The major work has grown around N,N-chelating pyridine bases and related species.[1−10] The number of heteroatoms, ring size, and the substituents in the heterocycle ring significantly modify the $\pi$-acidity and regulate the physical and chemical properties of the compounds.[11]

In search for other N-heterocycles, imidazole is chosen at first because it is a ubiquitious ligand in chemical and biological molecules and appears as such in biomolecules such as proteins and nucleic acids.[12−15] Recently the design of molecular architectures with imidazole has aroused interest in understanding biomolecular interactions with metal ions in biology and providing models for the active sides of metalloproteins.[12−15] In comparison to the progress in the chemistry of ruthenium−pyridine/its derivatives, ruthenium−imidazole and derivatives chemistry has been very slow.[15] Ruthenium−imidazole complexes are of interest for their antitumor activities.[15]

Ligands consisting of one pyridine ring with a pendent nitrogen donor from an azo function, known as (arylazo)-pyridines (aap, **1**) (Chart 1), have been employed very recently in the development of transition metal coordination chemistry.[7,8,16] Due to unsymmetric N-donor sites in the azo imine function, −N═N−C═N−, isomeric complexes in ruthenium and osmium have been extensively studied.[4−8] But a similar chemistry of (arylazo)imidazoles (**2**) is scarce in the literature.[17] Besides, the azo group is one of the potential functional units[18] which may be photochromatic, pH-responsive, redox active, and mediate electronic communications between photoredox active groups. With this background we have initiated research on ruthenium chelates of (arylazo)imidazoles. The exobidentate[19] behavior of the imidazole group is restricted by N-alkylation,[20] giving a new series of ligands 1-alkyl-2-(arylazo)imidazoles (L, **3**/**4**) which behave as N,N-chelating systems. In this first report we describe the synthesis, spectra, redox properties, and single-crystal X-ray structures of the two isomers of the ruthenium(II) complexes $RuL_2Cl_2$ (where L is 1-methyl-2-(arylazo)-imidazole ($L_1$, **3**) and 1-benzyl-2-(arylazo)imidazole ($L_2$, **4**).

**Chart 1**

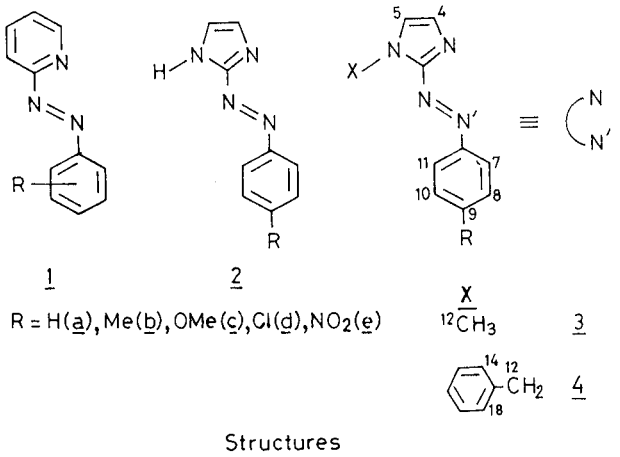


Structures

## Results and Discussion

**A. Ligands and Complexes.** 1-Methyl-2-(arylazo)imidazoles ($L_1$, **3**) (Chart 1) and 1-benzyl-2-(arylazo)imidazoles ($L_2$, **4**) are used as ligands. 2-(Arylazo)imidazoles (**2**) are synthesized by coupling aryldiazonium ions with imidazole in aqueous sodium carbonate solution (pH 7) and purified by the reported method.[21] The alkylation is carried out by adding alkyl halide in dry THF solution to the corresponding 2-(arylazo)imidazole in the presence of sodium hydride.[20] The ligands are new and act as N,N-chelating molecules. The donor centers are abbreviated as N(imidazole), N, and N(azo), N′. The atom-numbering scheme is shown in the structures (**3**/**4**).

An ethanolic solution of L reacts with $RuCl_3$ under dinitrogen and affords the complexes $RuL_2Cl_2$ via spontaneous reductive chelation. From the cooled reaction mixture, dark colored crystals are collected in high yield. On chromatographic separation (see below), major green (isomer (i) (**5**/**6**)) and minor blue (isomer (iii) (**7**/**8**)) products are obtained (see Chart 2). From the mother liquor major blue isomer (iii) is isolated. Even when L is used in excess of 2 mol, only $RuL_2Cl_2$ is isolated from this reaction.

The pseudooctahedral dichloro species of type $RuL_2Cl_2$, considering the unsymmetric bidentate chelation, 1-alkyl-2-(arylazo)imidazole (NN′), can in principle occur in five geo-

(10) Lincoln, P.; Nordén, B. *J. Chem. Soc., Chem. Commun.* **1996**, 2145. Nordén, B.; Lincoln, P.; Akerman, B.; Tusite, E. In *Metal Ion Complexes of Small Molecules*; Sigel, A., Sigel, H., Eds.; Marcel Decker: New York, 1996; Vol. 33, p 177. Good-fellow, B. J.; Felix, V.; Pacheco, S. M. D.; de Jesus, J. P.; Drew, M. G. B. *Polyhedron* **1997**, *16*, 393. Dupureur, C. M.; Barton, J. K. *Inorg. Chem.* **1997**, *36*, 33.

(11) Constable, E. C. *Coord. Chem. Rev.* **1989**, *93*, 205. Yamamoto, T.; Zhou, Z.; Kanbara, T.; Shimura, M.; Kizu, K.; Maruyama, T.; Takamura, T.; Fukuida, T.; Lee, B.; Ooba, N.; Tomaru, S.; Kurihara, T.; Kaino, T.; Kubota, K.; Sasaki, S. *J. Am. Chem. Soc*. **1996**, *118*, 10389.

(12) Higgis, T. C.; Helliwell, M.; Garner, C. D. *J. Chem. Soc., Dalton Trans.* **1996**, 2101. Halz, R. C.; Gobena, F. T. *Polyhedron* **1996**, *15*, 2779. Abe, J.; Shirai, Y. *J. Am. Chem. Soc*. **1996**, *118*, 4705. Tejel, C.; Villiarroya, B. F.; Ciriano, M. A.; Oro, A.; Lanfranchi, M.; Tiripicchio, A.; Camellini, M. T. *Inorg. Chem.* **1996**, *35*, 4360. Rodriquer, M. C.; Badaraus, I. M.; Cesario, M.; Guilhem, J.; Keita, B.; Nadjo, L. *Inorg. Chem.* **1996**, *35*, 7804. Sigel, H., Ed. *Metal Ions in Biological System*; Marcel Dekker: New York, 1981; Vol. 13.

(13) (a) Melnik, M.; Macaskova, L.; Holloway, C. E. *Coord. Chem. Rev.* **1993**, *126*, 71. (b) Matthews, C.; Clegg, W.; Elsegood, M. R. J.; Leese, T. A.; Thorp, D.; Thornton, P.; Lockhart, J. C. *J. Chem. Soc., Dalton Trans*. **1996**, 1531. (c) Rajan, R.; Rajaram, R.; Nair, B. U.; Ramasami, T.; Mondal, S. K. *J. Chem. Soc., Dalton Trans.* **1996**, 2019. (d) Baumann, T. F.; Nasir, M. S.; Sibert, J. W.; White, A. J. P.; Olmstead, M. M.; Williams, D. J.; Barrett, A. G. M.; Hoffman, B. M. *J. Am. Chem. Soc.* **1996**, *118*, 10479. (e) Liu, J. C.; Wang, S. X.; Wang, L. F.; He, F. Y.; Huang, X. Y. *Polyhedron* **1996**, *15*, 3659. (f) Luneau, D.; Risoan, G.; Rey, P.; Grand, A.; Caneschi, A.; Gatteschi, D.; Laugier, G. *Inorg. Chem.* **1993**, *32*, 5616.

(14) Belanger, S.; Beauchamp, A. L. *Inorg. Chem*. **1996**, *35*, 7836.

(15) Anderson, C.; Beauchamp, A. L. *Inorg. Chem.* **1995**, *34*, 6065. Hatcidimitriou, A.; Gourdon, A.; Devillers, J.; Launacy, J. P.; Mena, E.; Amouyal, E. *Inorg. Chem.* **1996**, *35*, 2215. Keppler, B. K.; Wehe, D.; Endres, H.; Rupp, N. *Inorg. Chem.* **1987**, *26*, 8440.

(16) Roy, R.; Chattopadhyay, P.; Sinha, C.; Chattopadhyay, S. *Polyhedron* **1996**, *15*, 3361. Pal, C. K.; Chattopadhyay, S.; Sinha, C.; Chakravorty, A. *Polyhedron* **1994**, *13*, 999. Ghosh, P.; Pramanik, A.; Bag, N.; Chakravorty, A. *J. Chem. Soc., Dalton Trans.* **1992**, 1883. Datta, D.; Chakravorty, A. *Inorg. Chem.*, **1983**, *22*, 1085. Ghosh, B. K.; Mukhopadhyay, A.; Goswami, S.; Ray, S.; Chakravorty, A. *Inorg. Chem.* **1984**, *23*, 4633−4639. Bandyopadhyay, P.; Bandyopadhyay, D.; Chakravorty, A.; Cotton, F. A.; Falvello, L. R.; Han, S. *J. Am. Chem. Soc.* **1983**, *105*, 6327.

(17) Mohamoud, M.; Hamman, A. H.; El-gyar, S. A. *Montash. Chem.* **1986**, *117*, 313. Cingolani, A.; Lorenzolti, A.; Leonesi, D.; Bondati, F. *Gazz. Chim. Ital.* **1981**, *111*, 243.

(18) Otsuki, J.; Sato, K.; Tsujino, M.; Okuda, N.; Araki, K.; Seno, M. *Chem. Lett.* **1996**, 847. Yam, V. W.-W.; Lau, V. C.-Y.; Cheung, K.-K. *J. Chem. Soc., Chem. Commun.* **1995**, 259. Marvand, V.; Launary, J. P. *Inorg. Chem.* **1993**, *32*, 1376. Das, A.; Maher, J. P.; McCleverty, J. A.; Badiola, J. A. N.; Ward, M. D. *J. Chem. Soc., Dalton Trans.* **1993**, 681.

(19) Masciocchi, N.; Moret, M.; Cairati, P.; Sironi, A.; Ardizzoia, G. A.; LaMonica, G. *J. Chem. Soc., Dalton Trans.* **1995**, 1671. Shyu, H. L.; Wei, H. H.; Lee, G. H.; Wang, T. *Inorg. Chem.* **1996**, *35*, 5396.

(20) Das, D.; Nayak, M. K.; Sinha, C. *Transition Met. Chem.* **1997**, *22*, 172.

(21) Fargher, R. G.; Pyman, L. *J. Chem. Soc.* **1991**, *115*, 217.

**Chart 2**

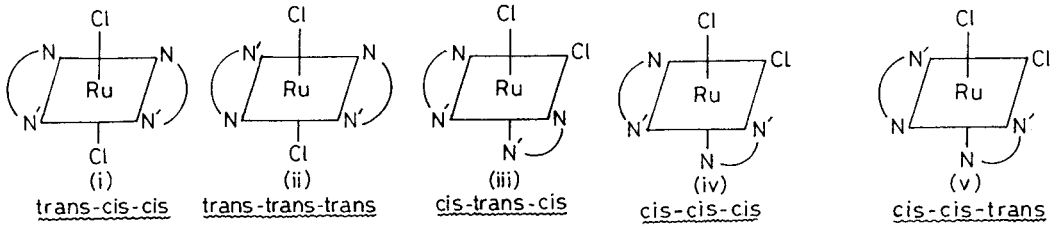


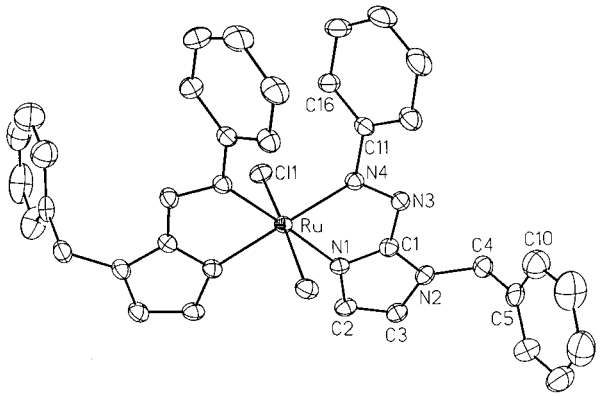


**Figure 1.** ORTEP plot and atom-labeling scheme for the *trans*−*cis*−*cis* compound (**6a**). All non-hydrogen atoms are represented by their 40% probability ellipsoids.

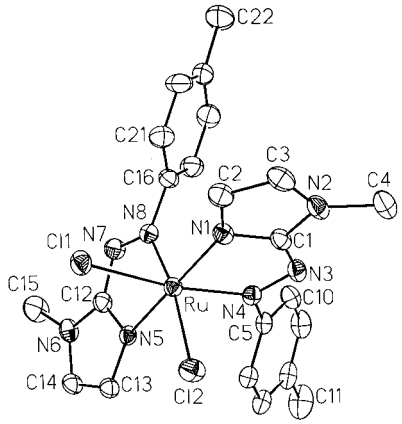


**Figure 2.** ORTEP plot and atom-labeling scheme for the *cis*−*trans*−*cis* compound (**7b**). All non-hydrogen atoms are represented by their 40% probability ellipsoids.

metrically isomeric forms.[6,7h] Two (i, ii) and three (iii−v) of these respectively have the $RuCl_2$ group in trans and cis geometries. If the coordinating pairs of Cl, N, and N′ are considered in that order, the configurations of these five are *trans*−*cis*−*cis* (i), *trans*−*trans*−*trans* (ii), *cis*−*trans*−*cis* (iii), *cis*−*cis*−*cis* (iv), and *cis*−*cis*−*trans* (v). Of these, two isomers, the green, *trans*−*cis*−*cis* (i) (**5**/**6**) and the blue, *cis*−*trans*−*cis* (iii) (**7**/**8**) are isolated and characterized by spectroscopic data. A definitive assignment based on the three-dimensional X-ray structure determination of these two isomers is reported here. The green isomer is quantitatively converted to blue isomer iii on refluxing in a high boiling solvent like, 1,2-dichlorobenzene.

**B. Molecular Structures.** Views of the molecular units of green **6a** and blue **7b** are given in Figures 1and 2, respectively. The coordination around ruthenium is approximately octahedral. The atomic arrangement in **6a** involves sequentially two *trans*-chlorines, *cis*-N(imidazole)s (N), and *cis*-N(azo)s (N′) and corresponds to a *trans*−*cis*−*cis* configuration. Similarly, the arrangement in **7b** is *cis*−*trans*−*cis*.

**Green Isomer, 6a.** The two atomic groups Ru, Cl(1), N(1a), N(4), Cl(1a) and Ru, Cl(1), N(1), Cl(1a), N(4a) separately constitute two excellent planes (mean deviation 0.03 Å and dihedral angle 76.5°) and are orthogonal to the third molecular plane Ru, N(1), N(4), N(4a), N(1a) (mean deviation 0.02 Å). The N(1)−Ru−N(4) angle is 177.5(1),° which is distorted from linearity by 2.5°. This deviation originates undoubtedly from the acute (76.4(1)°) chelate bite angle. The chelate ring is deviated from the mean plane by 0.05 Å and inclined at an angle 4.1° with $RuN_4$ plane. The phenylazo plane makes an angle 50.8° with the chelated azoimine fragment and suggests stereochemically nonequivalent C−H functions. Two *cis*-phenylazo planes are also not parallel, and the dihedral angle is 11.1°. The *trans*-chlorine angle is 174.8(1)° and is corroborated with a distorted octahedral structure.

The Ru−N′ (N(azo): N(4) or N(4a)) bond (2.016(3) Å) is shorter than the Ru−N (N(imidazole): N(1) or N(1a)) (2.063(3) Å) bond distance by 0.05 Å. The shortening may be due to greater $\pi$-back-bonding, $d\pi(Ru) \rightarrow \pi^*(azo)$.[7,8] The N−N distance is not available in the free ligand. However, the data available in some free azo ligands suggest that it is nearly 1.25 Å.[8b] In the complex the N−N distance is 1.229(5) Å. The coordination can lead to a decrease in the N−N bond order due to both $\sigma$-donor and $\pi$-acceptor character of the ligands—the latter character having more pronounced effect and possibly being the reason for elongation. The selected bond parameters are listed in Table 1.

**Blue Isomer, 7b.** The two atomic groups Ru, Cl(1), N(5), N(4), N(1) (mean deviation 0.01 Å) and Ru, Cl(2), N(5), N(8) (mean deviation 0.03 Å) constitute two orthogonal (dihedral angle 91.1°) planes. On the other hand, the planarity of the atomic group Ru, Cl(1), Cl(2), N(4), N(8) is not good (mean deviation 0.2 Å) due to relatively large deviations of N(4) and N(8) from the best plane in opposite directions. The *trans*-angles around the Ru center in the planes range from 169.6(1) to 176.9(1)° indicating distortions from the rectilinear geometry. The chelate angles extended by azoimidazoles are 76.7(1) and 76.9(1)° and are considerably deviated from the ideal geometry. As a consequence of the constraint of the bite angle, the ligands are bent back from the coordinated chlorides. It is remarkable that most of the distortions away from the octahedral positions arise out of the small bite angle and are associated with the azo nitrogens whereas the imidazole nitrogens occupy nearly axial positions [N(1)−Ru−N(5) = 176.9(1)°]. Each chelate ring is a good plane with no atom deviating by more than 0.06 Å. The dihedral angles between the chelate ring and the corresponding *p*-tolyl ring are 53.4 and 56.7°. The *cis*-chloro angle of 91.1-(1)° is very nearly the ideal octahedral angle and is comparable to reported values.[2c,7f] Two chelate planes are deviated from orthogonality (dihedral angle 95.8°) possibly due to steric interaction.

The N−N distance is comparatively longer than that of isomer **6a** by ∼0.01 Å. The Ru−N(imidazole) (2.033(4), 2.043(4) Å) distance is longer than Ru−N(azo) (1.991(4), 1.987(4) Å) and

**Table 1.** Selected Bond Distances (Å) and Angles (deg) and Their Estimated Standard Deviations for (i) **6a** and (ii) **7b**

(i) *Trans*−*Cis*−*Cis*: ($C_{38}H_{34}N_8Cl_2Ru$ (**6a**))

Distances

| | | | |
|---|---|---|---|
| Ru−N(1) | 2.063(3) | C(1)−N(1) | 1.325(5) |
| Ru−N(4) | 2.016(3) | C(1)−N(3) | 1.369(5) |
| Ru−Cl(1) | 2.382(2) | N(3)−N(4) | 1.299(5) |

Angles

| | | | |
|---|---|---|---|
| N(1)−Ru−N(4) | 76.4(1) | Cl(1)−Ru−Cl(1A) | 174.8(1) |
| N(1)−Ru−Cl(1A) | 86.5(1) | N(4)−Ru−N(4A) | 105.7(2) |
| Ru−N(1)−C(1) | 109.9(2) | N(4)−N(3)−C(1) | 109.3(3) |
| Ru−N(4)−N(3) | 120.2(2) | Ru−N(4)−C(11) | 129.5(3) |
| N(1)−Ru−N(1A) | 101.4(2) | N(1)−Ru−Cl(1) | 90.3(1) |
| N(4)−Ru−Cl(1) | 92.2(1) | N(1)−Ru−N(4A) | 177.5(1) |
| N(4A)−Ru−Cl(1) | 91.0(1) | | |

(ii) *Cis*−*Trans*−*Cis* ($C_{22}H_{24}N_8Cl_2Ru$ (**7b**))

Distances

| | | | |
|---|---|---|---|
| Ru−N(1) | 2.033(4) | N(1)−C(1) | 1.330(6) |
| Ru−N(5) | 2.043(4) | N(3)−C(1) | 1.351(5) |
| Ru−N(4) | 1.991(4) | N(4)−C(5) | 1.426(5) |
| Ru−N(8) | 1.987(4) | N(5)−C(12) | 1.331(6) |
| Ru−Cl(1) | 2.392(2) | N(7)−C(12) | 1.358(6) |
| Ru−Cl(2) | 2.407(2) | N(8)−C(16) | 1.438(6) |
| N(3)−N(4) | 1.307(5) | N(2)−C(4) | 1.469(7) |
| N(7)−N(8) | 1.301(5) | N(6)−C(15) | 1.451(7) |

Angles

| | | | |
|---|---|---|---|
| N(1)−Ru−N(4) | 76.9(1) | Ru−N(8)−N(7) | 120.6(3) |
| N(5)−Ru−N(8) | 76.7(1) | N(8)−N(7)−C(12) | 108.9(4) |
| N(1)−Ru−Cl(1) | 92.7(1) | N(7)−C(12)−N(5) | 122.5(4) |
| N(1)−Ru−Cl(2) | 89.1(1) | C(12)−N(5)−Ru | 109.6(3) |
| N(4)−Ru−Cl(1) | 169.6(1) | Ru−N(4)−N(3) | 120.3(3) |
| N(4)−Ru−Cl(2) | 90.0(1) | N(4)−N(3)−C(1) | 109.2(4) |
| N(1)−Ru−N(8) | 101.0(1) | N(3)−C(1)−N(1) | 122.6(4) |
| N(4)−Ru−N(5) | 101.0(1) | Ru−N(1)−C(1) | 110.4(3) |
| N(8)−Ru−Cl(2) | 169.7(1) | N(1)−Ru−N(5) | 176.9(1) |
| Ru−N(8)−C(16) | 126.7(3) | Ru−N(4)−C(5) | 126.0(3) |

is the indication of an M−L $\pi$-interaction that is localized in the M−azo fragment. The Ru−Cl distance is comparable with the reported values.[7f] The bond parameters are given in Table 1.

**C. Spectra.** Sharp intense single bands at 1400−1415 $cm^{-1}$ corresponding to $\nu_{N=N}$ in the ligands (L) are shifted to 1270−1320 $cm^{-1}$ in the complexes. The low-energy shifting is an indication of N-coordination and may be attributed to Ru(d$\pi$) → $\pi$* charge transitions.[6−8] Green $RuL_2Cl_2$ display an intense, sharp, single stretch at 325−340 $cm^{-1}$ assignable to $\nu_{Ru-Cl}$, and the blue isomers exhibit two similar stretches at 310−320 $cm^{-1}$ in agreement with the *cis*-$RuCl_2$ configuration.

UV−visible spectral studies of the complexes exhibit absorptions at 250−900 nm (Table 2). The allowed transitions at nearly 400 nm are probably of ligand origin and are not considered further. The green complexes (**5**, **6**) show an intense ($\epsilon \sim 10^4$) band in the region 675 ± 15 nm and is assigned to the $t_2$(Ru) → $\pi$*(L) transition (MLCT), where the $\pi$* level has large azo character.[4−8] The blue isomers (**7**/**8**) have an intense ($\epsilon \sim 10^4$) absorption at 590 ± 10 nm with a weak shoulder ($\epsilon \sim 10^3$) at 870 ± 10 nm. The more intense band at higher energy is believed to be the spin-allowed singlet−singlet transition while the weaker band at lower energy could be the corresponding singlet−triplet transion made particularly, allowed by the strong spin−orbit coupling in ruthenium.[23] Other transition probabilities like low-symmetry splitting of the metal level and the presence of more than one interacting ligand (each contributing one $\pi$* orbital) are excluded due to a small extinction coefficient.[24]

The $^1$H NMR spectra of the ligands and complexes are compared to determine the binding mode and stereochemistry of the complexes. The alkylation of azoimidazoles was supported by the disappearance of $\delta_{N-H}$ at ∼ 10.4 ppm and the appearance of an alkyl signal in the aliphatic region.[20] The N−Me and methylenic N−$CH_2$ Ph appear as singlets at 4.00 ppm for **3** and 5.6 ppm for **4**, respectively. The imidazolic 4- and 5-H protons appear at 7.2−7.3 and 7.1−7.2 ppm, respectively. 2-Aryl protons (7−11-H) appear at 7−8.2 ppm, and the signal movement is in accordance with the inductive and electronic effect of the substituents.[26]

The N−Me signal appears at 4.2 and 4.1 ppm in the green (**5**) and blue (**7**) complexes, respectively. The methylene N−$CH_2$ Ph appears as a singlet at 5.7 ppm in the green complexes (**6**) while it gives AB type quartets at 5.4 and 5.7 ppm in the blue complexes (**8**). The geminal coupling constant[25] is 16 Hz. There are, however, neither neighboring chiral centers nor any appreciable bond rotational barriers, but there does exist a distorted coordination around the metal. This overall distortion leads to the molecular dissymmetry. The appearance of single Ar−$CH_3$ and Ar−$OCH_3$ signals in the complexes is also supported by earlier work on ruthenium(II) and osmium(II) (arylazo)pyridine complexes.[7g,8] The ligand binding to ruthenium(II) is supported by downfield shifting of N−R signals by 0.1−0.2 ppm. The aryl protons 8,10- (8′, 10′-) H resonate symmetrically at a single position, and 7- (7′-) and 11- (11′-) H resonate asymmetrically indicative of a magnetically different environment. The 11- (11′-) H is assigned as stereochemically nearer than 7- (7′-) H to the metal center. In the blue complexes (**7**, **8**) the steric effect induces more distortion, which is reflected in the greater separation in signal resonances of 11- (11′-) H and 7- (7′-) H. The separation is less than 20 Hz in green and greater than 50 Hz in the blue isomers.

**D. Redox Studies and Correlation with Electronic Spectra.** The redox behavior of the complexes in acetonitrile solution was examined cyclic voltammetrically at a platinum disk working electrode and the potentials are reported with reference to the SCE. The voltamograms display metal oxidations at the positive side and the ligand reductions at the negative side to the SCE. The results are in Table 2, and a representative voltamogram is shown in Figure 3.

In the potential range +0.5 to +2.0 V at the scan rate 50 mV $s^{-1}$ in acetonitrile one reversible to quasireversible (peak-to-peak separation $\Delta E_p$ = 60−80 mV) oxidative response[7,8] is observed corresponding to the couple (1).

$$RuL_2Cl_2^{+} + e \rightleftharpoons RuL_2Cl_2 \qquad (1)$$

The data (Table 1) reveal that the complexes **7** and **8** exhibit higher redox potentials by 0.1−0.2 V than that of green complexes **5** and **6**. In **7** and **8** two azo functions are *cis*-oriented and back-bonding interactions may in turn occur with two different d$\pi$ orbitals, and in **5** and **6** the *trans*−oriented azo will compete for the same d$\pi$ orbital. This may lead to an increase in effective charge on ruthenium in **7** and **8** and may shift the ruthenium(III)/ruthenium(II) couple to more positive values than for **5** and **6**. The potential is sensitive to the

(22) Lockhart, J. C.; Rushton, D. J. *J. Chem. Soc., Dalton Trans.* **1991**, 2633.
(23) (a) Kober, E. M.; Meyer, T. J. *Inorg. Chem.* **1982**, *21*, 3967. (b) Decurtines, S.; Felix, F.; Ferguson, J.; Gudel, H. U.; Ludi, A. *J. Am. Chem. Soc.* **1980**, *102*, 4102.
(24) Pankuch, B. J.; Lacky, D. E.; Crosby, G. A. *J. Phys. Chem.* **1989**, *84*, 2061. Ceulemans, A.; Vanquickenborne, L. G. *J. Am. Chem. Soc.* **1981**, *103*, 2238.
(25) (a) Chattopadhyay, S.; Sinha, C.; Basu, P.; Chakravorty, A. *J. Organomet. Chem.* **1991**, *414*, 421. (b) Sinha, C. *Polyhedron* **1993**, *12*, 2363.

**Table 2.** UV−Vis Spectral[a] and Cyclic Voltammetric Data[b−d]

| compd | $\nu_{max}$, nm ($10^{-3}\epsilon$, $M^{-1}$ $cm^{-1}$) | | | | $\nu_{CT}$ (eV) | Ru(III)/Ru(II) $E_M^0$, V ($\Delta E_p$, V) | azo$^-$/azo $-E_L^0$, V ($\Delta E_p$, V) | ($\Delta E°$, (V) |
|---|---|---|---|---|---|---|---|---|
| **5a** | 664 (12.11) | 395 (10.57) | 333 (13.69) | | 1.869 | 0.614 (0.072) | 0.834 (0.101) | 1.448 |
| **5b** | 662 (12.11) | 414 (12.31) | 342 (15.38) | | 1.875 | 0.581 (0.065) | 0.872 (0.082) | 1.453 |
| **5c** | 661 (7.86) | 450 (11.98) | 348 (12.24) | | 1.877 | 0.560 (0.068) | 0.901 (0.110) | 1.461 |
| **5d** | 669 (10.56) | 386 (13.33) | 346 (15.48) | | 1.855 | 0.666 (0.074) | 0.753 (0.120) | 1.419 |
| **5e** | 680 (9.07) | 400 (8.86) | 345 (11.21) | | 1.825 | 0.764 (0.070) | 0.610 (0.084) | 1.374 |
| **6a** | 660 (12.53) | 409 (10.06) | 340 (13.92) | | 1.88 | 0.643 (0.080)[e] | 0.788 (0.076) | 1.431 |
| **6b** | 668 (10.73) | 416 (10.03) | 344 (13.31) | | 1.858 | 0.611 (0.075)[e] | 0.844 (0.110) | 1.455 |
| **6c** | 661 (13.75) | 444 (15.88) | 349 (13.31) | | 1.875 | 0.591 (0.065)[e] | 0.878 (0.110) | 1.469 |
| **6d** | 674 (11.74) | 405 (10.72) | 339 (14.67) | | 1.841 | 0.698 (0.070)[e] | 0.685 (0.120) | 1.383 |
| **6e** | 685 (10.50) | 404 (9.89) | 348 (12.59) | | 1.812 | 0.802 (0.070)[e] | 0.498 (0.090) | 1.300 |
| **7a** | 865 (1.25)[f] | 588 (10.87) | 376 (15.85) | 343 (17.01) | 2.110 | 0.777 (0.080) | 0.828 (0.120) | 1.605 |
| **7b** | 858 (0.97)[f] | 590 (11.15) | 382 (22.15) | 340 (24.39) | 2.103 | 0.746 (0.070) | 0.868 (0.110) | 1.614 |
| **7c** | 856 (1.02)[f] | 588 (10.95) | 380 (18.29) | 338 (21.18) | 2.111 | 0.723 (0.075) | 0.919 (0.095) | 1.642 |
| **7d** | 868 (1.20)[f] | 592 (9.97) | 376 (20.32) | 335 (23.49) | 2.100 | 0.805 (0.075) | 0.782 (0.122) | 1.587 |
| **7e** | 864 (1.00)[f] | 610 (9.73) | 377 (25.02) | 340 (28.90) | 2.034 | 0.891 (0.080) | 0.618 (0.110) | 1.509 |
| **8a** | 870 (1.10)[f] | 580 (9.97) | 377 (20.12) | 338 (24.31) | 2.140 | 0.803 (0.078) | 0.798 (0.114) | 1.601 |
| **8b** | 861 (1.36)[f] | 593 (10.38) | 382 (22.14) | 335 (25.01) | 2.093 | 0.759 (0.085) | 0.841 (0.103) | 1.600 |
| **8c** | 860 (1.25)[f] | 590 (10.22) | 385 (21.41) | 340 (23.15) | 2.103 | 0.742 (0.080) | 0.874 (0.102) | 1.616 |
| **8d** | 866 (1.43)[f] | 594 (10.24) | 377 (21.67) | 335 (24.19) | 2.089 | 0.827 (0.085) | 0.749 (0.117) | 1.576 |
| **8e** | 866 (1.88)[f] | 604 (10.76) | 375 (23.14) | 346 (27.58) | 2.055 | 0.920 (0.083) | 0.619 (0.104) | 1.539 |

[a] In $CH_3CN$. [b] Meaning and units of the symbols are the same as in text. [c] Solvent is $CH_3CN$. [d] Supporting electrolyte TBAP(0.01 M), solute concentration $10^{-3}$ M; scan rate is 0.05 V $s^{-1}$. [e]Quasireversible Ru(IV)/Ru(III): $E_{pa}$ = 1.142 (**6a**), 1.125 (**6b**), 1.115 (**6c**), 1.152 (**6d**), and 1.449 (6e) V. [f]Shoulder.

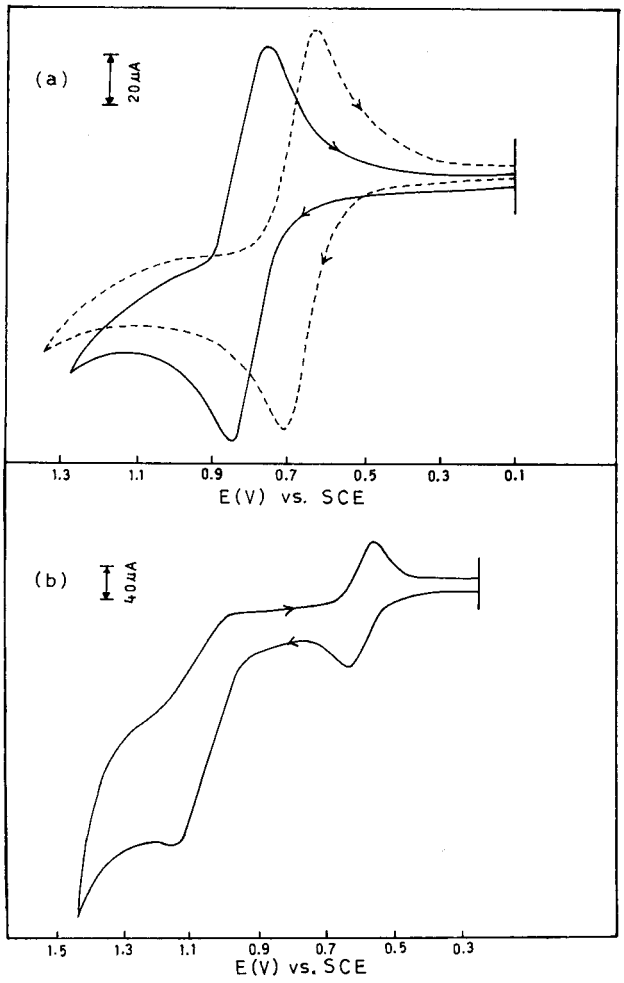


**Figure 3.** 3. Cyclic voltammograms in acetonitrile (0.1 M TBAP) at a platinum working electrode. The solute concentration and scan rate are ~$10^{-3}$ M and 50 mV $S^{-1}$, respectively: (a) *trans*−*cis*−*cis* (**5d**) (•••) *cis*−*trans*−*cis* (**7d**) (- - -); (b) *trans*−*cis*−*cis* (**6b**).

substituents both at the aryl ring and imidazole N(1)-position. The green complexes (**6**) exhibit two successive oxidative responses in which the first one refers to couple (1) and the quasireversible second response ($\Delta E_p$ = 90−120 mV) may correspond to the ruthenium(IV)/ruthenium(III) couple (2).

$$RuL_2Cl_2^{2+} + e \rightleftharpoons RuL_2Cl_2^{+} \qquad (2)$$

The ruthenium(III)/ruthenium(II) redox potential of the present examples falls between the potentials of bipyridine[27] and azopyridine complexes.[7] This is corroborated with the $\pi$-acidity order[11] of the ligands such as bipyridine < azoimidazole < azopyridine. The azoimidazole ligands thus stabilize (with respect to oxidation) ruthenium(II) better than bipyridine but less effectively than azopyridines.

In the potential range 0.0 to −1.5 V reductive responses are observed under similar conditions. The reduced species appears to be less stable, and on scan reversal, multiple anodic responses are observed. The reduction may be due to the azo function analogous to the azopyridine systems. The LUMO of L can accommodate up to two electrons and the reduction may be represented by (3). A decrease in the $\sigma$-donor capacity of the

$$-N{=}N- \overset{+e}{\rightleftharpoons} [-N\cdots N-]^- \overset{+e}{\rightleftharpoons} [-N{-}N-]^{2-} \qquad (3)$$

substituent in the ligand frame increases both the ruthenium(III)/ruthenium(II) and the first bound-ligand reduction potentials.[4] The two potentials correlate linearly with the slope less than unity. The observation may be rationalized as follows. A decrease in $\sigma$-donor capacity stabilizes ligand $\pi$ orbitals and increases the effective charge on ruthenium, and this in turn stabilizes metal d$\pi$-orbitals indirectly. Subsequently, d$\pi$* back-bonding further destabilizes ligand $\pi$* orbitals and stabilizes the metal d$\pi$-orbitals.[28] The extent of perturbation is found to be more pronounced in the ligand $\pi$* orbitals (slope of $E_M^0$ vs $E_L^0$ plot is less than unity), which may be due to direct bonding

(26) (a) Chattopadhyay, P.; Sinha, C. *Polyhedron*, **1994**, *13*, 2689. (b) Jackman, L. M. *Applications of Nuclear Magnetic Resonance Spectroscopy in Organic Chemistry*; Pergamon Press: New York, 1959.
(27) Johnson, E. C.; Sullivan, B. P.; Salmon, D. J.; Adeyemi, S. A.; Meyer, T. J. *Inorg. Chem.* **1978**, *17*, 2211.
(28) Rillema, D. P.; Allen, G.; Meyer, T. J.; Conard, D. *Inorg. Chem.* **1983**, *22*, 1617.

**Table 3.** Comparison of Spectral and Redox Properties of $Ru(aap)_2Cl_2$ and $RuL_2Cl_2$

| | $Ru(aap)_2Cl_2$ | | $RuL_2Cl_2$ | |
|---|---|---|---|---|
| | green (*trans*−*trans*−*trans*) | blue (*cis*−*trans*−*cis*) | green (*trans*−*cis*−*cis*) | blue (*cis*−*trans*−*cis*) |
| Ru(III)/Ru(II) couple, $E^\circ_{298}$ (V) | 0.90−0.95 | 1.10 | 0.6−0.7 | 0.7−0.9 |
| MLCT bands, $\lambda_{max}$ (nm) | 635 | 580 | 665 | 590 |

of the substituent in the ligand frame.[29] The difference in two successive redox properties positive and negative to SCE ($\Delta E^\circ = E_M{}^0(1) - E_L{}^0(3)$) may be correlated with the MLCT transition. The electronic excitation may be considered as intramolecular redox process, and the energy $\nu_{CT}$ of the lowest MLCT transition is expected to be linearly related with $\Delta E^\circ$ (Table 1). The least-squares plot of $\nu_{CT}$ (in eV) against $\Delta E^\circ$ (V) corresponds to eq 4. A similar correlation has been observed for bpy[30] and ((arylazo)pyridine)ruthenium complexes.[4]

$$\nu_{CT} = 1.19\ \Delta E^\circ + 0.18 \qquad (4)$$

**E. Comparison with Azopyridine Analogues.** (Arylazo)-pyridines (**1**) and (arylazo)imidazoles (**3/4**) belong to the azo imine, −N═N−C═N−, family of heterocyclic nitrogenous compounds. The steric and electronic properties of the imidazole ring may be regulated by N(1)-substitution, and the appearance of the ring as such in biomolecules make the azoimidazoles more versatile ligands than azopyridines. The present class of molecules have intermediate $\pi$-acidity in comparison with bipyridine and azopyridines. Thus the electronic and redox properties of ruthenium(II) complexes lie between $Ru(bpy)_2Cl_2$ and $Ru(aap)_2Cl_2$. The green isomer in $Ru(aap)_2Cl_2$ is suggested to have the *trans*−*trans*−*trans* configuration,[4,7j] while the $RuL_2Cl_2$ is *trans*−*cis*−*cis* as is established by three-dimensional X-ray structure determination. Two isomers of the *cis*−$RuCl_2$ configuration are structurally known[7f] as *cis*−*trans*−*cis* and *cis*−*cis*−*cis* in $Ru(aap)_2Cl_2$, but in the present case we are able to isolate one isomer (*cis*−*trans*−*cis*) only. The spectral and redox properties of the isomers compared in the Table 3. The data reveal that the ruthenium(III)/ruthenium(II) couple is shifted to more positive potential and the MLCT bands are blue shifted on going from azoimidazole to azopyridine−ruthenium(II) complexes. This is because of the decreased $\pi$-acidity of the five-membered heterocycle imidazole compared to the six-membered pyridine.[11]

## Experimental Section

**Materials.** 2-(Arylazo)imidazoles were prepared by the reported procedure.[21] Ruthenium trichloride was treated before use as earlier.[7] The purification of acetonitrile and preparation of tetrabutylammonium perchlorate (TBAP) for electrochemical work were done as before.[7] Dinitrogen was purified by bubbling through an alkaline pyrogallol solution. All other chemicals and solvents were of reagent grade and were used without further purification. Commercially available SRL silica gel (60−120 mesh) was used for column chromatography.

**Instrumentation**. Spectroscopic data were obtained with use of following instruments: UV−vis spectra, Shimadzu 160A; IR spectra (KBr disk, 4000−200 $cm^{-1}$), Perkin-Elmer 783 spectrophotometers; $^1H$ NMR spectra, JEOL 100 and Brucker 200 MHz FTNMR spectrometers. Electrochemical measurements were done with use of computer-controlled PAR model 270 VERSTAT electrochemical instruments, using a platinum disk working electrode. All results were collected at 298 K and are referenced to the saturated calomel electrode (SCE) in acetonitrile. The reported potentials are uncorrected for junction potential.

**Table 4.** Crystallographic Data for **6a** and **7b**

| | **6a** | **7b** |
|---|---|---|
| empirical formula | $C_{38}H_{34}Cl_2N_8Ru$ | $C_{22}H_{24}Cl_2N_8Ru$ |
| fw | 774.7 | 572.5 |
| cryst system | monoclinic | monoclinic |
| space group | *C*2/*c* | $P2_1/n$ |
| *a*, Å | 15.680(8) | 9.547(6) |
| *b*, Å | 22.766(14) | 22.554(12) |
| *c*, Å | 11.473(5) | 11.748(8) |
| $\beta$, deg | 119.27(4) | 99.07(5) |
| *V*, Å$^3$ | 3573(3) | 2498(3) |
| *Z* | 4 | 4 |
| *T*, K | 295 | 295 |
| $\lambda$, Å | 0.710 73 | 0.710 73 |
| $\pi_{calcd}$, g $cm^{-3}$ | 1.440 | 1.522 |
| $\mu$(Mo K$\alpha$), $cm^{-1}$ | 6.2 | 8.7 |
| transm coeff[a] | 0.8832 | |
| params refined | 222 | 298 |
| *R*,[b] % | 3.59 | 3.15 |
| $R_w$[c] % | 4.38 | 4.51 |
| GOF[d] | 1.27 | 1.51 |

[a] Maximum value normalized to 1. [b] $R = \Sigma\ ||F_o| - |F_c||\Sigma/|F_o|$. [c] $R_W = [\Sigma w(|F_o| - |F_c|)^2/\Sigma w|F_o|^2]^{1/2}$; $w^{-1} = \sigma^2(|F_o|) + g|F_o|;^2$ g = 0.00030 for **6a** and $g = 0.00050$ for **7b**. [d] The goodness-of-fit is defined as $[w(|F_o| - |F_c|)^2/(n_0 - n_v)]^{1/2}$, where $n_0$ and $n_v$ denote the numbers of data and variables, respectively.

**Synthesis of Ligands.** The 1-alkylated-2-(arylazo)imidazoles (**3/4**) were synthesized from the corresponding 2-(arylazo)imidazoles (**2**) by reacting the latter with the respective alkyl halide in the presence of sodium hydride in dry THF. A representative case is detailed below. Available information on the N-alkylation of imidazole served as a guide for setting experimental conditions.[22]

**1-Methyl-2-(*p*-methylphenyl)azo)imidazole (3b).** To a dry THF solution (15 mL) of 2-((*p*-methylphenyl)azo)imidazole (**2b**) (1 g, 5.4 mM) was added NaH (50% paraffin) (0.30 g) in small portions, and the mixture was stirred under cold conditions with an ice bath for 0.5 h. Methyl iodide (0.8 g, 5.6 mM) was added slowly through a pressure equalizing system under stirring conditions for a period of 1 h and then allowed to warm for another 1 h. The solution was evaporated to dryness, extracted with chloroform, and washed with NaOH solution (10%, 10 mL, ×3) and finally by distilled water (20 mL, ×3). The chloroform extract was chromatographed over silica gel column (45 × 1 mL) prepared in benzene. The elution was performed by 19:1 benzene−acetonitrile. On slow evaporation in air, an orange crystalline product was obtained, which was then dried over $P_4O_{10}$ under *vacuum*. The N(1)-benzylated derivatives (**4**) were synthesized similarly by using benzyl bromide. The yields and melting points (°C) are as follows: **3a** (40%, 100 ± 2), **3b** (45%, 116 ± 1), **3c** (35%, gum), **3d** (39%, 160 ± 1), **3e** (50%, decomposed above 250 °C), **4a** (45%, 94 ± 2), **4b** (50%, 150 ± 1), **4c** (30%, gum), **4d** (42%, 162 ± 1), **4e** (50%, 176 ± 1).

**Preparation of Complexes. Dichlorobis [1-methyl-2-(phenylazo)-imidazole]ruthenium(II), $Ru(HaaiMe)_2Cl_2$ (5a, 7a).** Nitrogen gas was passed through a brown solution of $RuCl_3{\cdot}3H_2O$ (0.13 g, 0.5 mM) in 20 mL of ethanol. Then 0.2 g (1.08 mM) of **3a** in 5 mL of ethanol was added. The mixture was refluxed under nitrogen with magnetic stirring for 10 h. During this period the solution color turned to green to bluish green with a dark precipitate. The solution was cooled to room temperature, filtered, and washed thoroughly with water, ethanol, and finally diethyl ether. It was then dried in a vacuum desiccator over $P_4O_{10}$. The dried product was dissolved in a small volume of $CH_2Cl_2$ and was subjected to chromatography on a silica gel (60−120

(29) Elliott, C. M.; Hersheuhart, E. J. *J. Am. Chem. Soc.* **1982**, *104*, 7519.
(30) (a) Dodsworth, E. S.; Lever, A. B. P. *Chem. Phys. Lett.* **1986**, *124*, 152. (b) Ghosh, P.; Chakravorty, A. *Inorg. Chem.* **1984**, *23*, 2242.

mesh) column (30 × 1 mL). A green band was eluted by 9:1 benzene−acetonitrile. A blue band was eluted further by 2:1 benzene−acetonitrile. Crystals were obtained by complete evaporation of the eluted solution at room temperature. The yields were as follows: green product (**5a**), 0.16 g, 59.0%; blue product (**7a**), 0.03 g, 11.1%. The bluish green solution was evaporated and subjected to chromatography, and a small portion of the green part with a major blue product was obtained. A pink mass was remained at the top of the column.

Other complexes were prepared by following the identical procedure, and the yields were varied 50−65% for the green isomers (**5**, **6**) and 10−20% for the blue isomers (**7**, **8**).

**Isomer Conversion. Green → Blue.** This is a thermal isomerization process. A representative case is given here. The green isomer $Ru(MeaaiMe)_2Cl_2$ (**5b**) (0.2 g, 0.35 mM) was suspended in 1,2-dichlorobenzene (15 mL) and heated to reflux for 4 h (conversion was tested by TLC). The solution was filtered, and the residue was washed with diethyl ether. It was dissolved in $CH_2Cl_2$ and chromatographed as before. A very small green band was eluted by 9.:1 benzene−acetonitrile followed by a deep blue band in 2:1 benzene−acetonitrile. The solution was evaporated in air slowly, and dark shining blue crystals were deposited. The yield was 0.17 g (85%).

**X-ray Crystal Structure and Analysis.** Crystals suitable for X-ray work were grown by slow diffusion of hexane into dichloromethane solution at 298 K (crystal sizes: *trans*−*cis*−*cis* (**6a**), 0.38 × 0.25 × 0.30 $mm^3$; *cis*−*trans*−*cis* (**7b**), 0.20 × 0.25 × 0.32 $mm^3$). Data were collected on a Siemens R3m/v diffractometer with graphite-monochromated Mo Kα radiation ($\lambda$ = 0.710 73 Å) at 295 K. Crystal data and data collection parameters are listed in Table 4. Unit cell parameters are determined by the least-squares fit of 30 machine-centered reflections ($2\theta$ = 15−28°). Systematic absence led to the identification of space groups *C*2/*c* for **6a** and $P2_1/n$ for **7b**. Data were collected by the $\omega$ scan method over the $2\theta$ range 3−45°. Two check reflections were measured after every 98 reflections during data collections to monitor crystal stability and showed no significant intensity reduction. All data were corrected for Lorentz polarization, and an empirical absorption correction was done on the basis of azimuthal scans.[31] Of the2595 (**6a**) and 3705 (**7b**) unique reflections 2006 and 2711 with $I > 3\sigma(I)$ were used for the respective structure solutions. Data reduction and all calculations related to structure solution were carried out on a Micro VAX II computer with the SHELXTL PLUS Programs.[32] The position of the metal atom in *trans*−*cis*−*cis*−**6a** and *cis*−*trans*−*cis*−**7b** were determined by direct and Patterson heavy atom methods, respectively. All non-hydrogen atoms wee located from subsequent difference Fourier maps. The hydrogen atoms were included at calculated positions with fixed thermal parameters ($U$ = 0.08 $Å^2$).

**Acknowledgment.** We are thankful to the Council of Scientific and Industrial Research and Department of Science and Technology, New Delhi, for financial support. The University Grants Commission provided a fellowship to D.D. Crystallography was performed at the National Single Crystal Diffractometer Facility, Department of Inorganic Chemistry, Indian Association for the Cultivation of Science. Our sincere thanks are due to Dr. B. B. De, University of Nottingham, Nottingham, U.K., for recording some $^1$H NMR spectra.

**Supporting Information Available:** Tables SI−SXII, listing anisotropic displacement coefficients, complete bond distances and angles, H coordinates and *U* values, atom coordinates and equivalent isotropic displacement coefficients, and the elemental (C, H, N) analysis, IR, and $^1$H NMR data for all the ligands and complexes, and UV−vis and $^1$H NMR spectra of **6b** and **8b** (14 pages). Ordering information is given on any current masthead page.

IC970446P

(31) North, A. C. T.; Phillips, D. C.; Mahtews, F. S. *Acta Crystallogr.* **1968**, *A24*, 351.
(32) Sheldrick, G. M. *SHELXTL-PLUS 88, Structure Determination Software Programs*; Nicolet Instrument Corp.: Madison, WI, 1988.